A retinal circuit for the suppressed-by-contrast receptive field of a polyaxonal amacrine cell

Yu Jia[a,b], Seunghoon Lee[a], Yehong Zhuo[b,1], and Z. Jimmy Zhou[a,c,d,1]

[a]Department of Ophthalmology and Visual Science, Yale University School of Medicine, New Haven, CT 06510; [b]State Key Laboratory of Ophthalmology, Zhongshan Ophthalmic Center, Sun Yat-Sen University, Guangzhou 510060, China; [c]Department of Cellular and Molecular Physiology, Yale School of Medicine, New Haven, CT 06510; and [d]Department of Neuroscience, Yale School of Medicine, New Haven, CT 06510

Edited by Thomas D. Albright, The Salk Institute for Biological Studies, La Jolla, CA, and approved February 24, 2020 (received for review August 3, 2019)

Amacrine cells are a diverse population of interneurons in the retina that play a critical role in extracting complex features of the visual world and shaping the receptive fields of retinal output neurons (ganglion cells). While much of the computational power of amacrine cells is believed to arise from the immense mutual interactions among amacrine cells themselves, the intricate circuitry and functions of amacrine–amacrine interactions are poorly understood in general. Here we report a specific interamacrine pathway from a small-field, glutamate–glycine dual-transmitter amacrine cell (vGluT3) to a wide-field polyaxonal amacrine cell (PAS4/5). Distal tips of vGluT3 cell dendrites made selective glycinergic (but not glutamatergic) synapses onto PAS4/5 dendrites to provide a center-inhibitory, surround-disinhibitory drive that helps PAS4/5 cells build a suppressed-by-contrast (sbc) receptive field, which is a unique and fundamental trigger feature previously found only in a small population of ganglion cells. The finding of this trigger feature in a circuit upstream to ganglion cells suggests that the sbc form of visual computation occurs more widely in the retina than previously believed and shapes visual processing in multiple downstream circuits in multiple ways. We also identified two different subpopulations of PAS4/5 cells based on their differential connectivity with vGluT3 cells and their distinct receptive-field and luminance-encoding characteristics. Moreover, our results revealed a form of crosstalk between small-field and large-field amacrine cell circuits, which provides a mechanism for feature-specific local (<150 μm) control of global (>1 mm) retinal activity.

retinal circuitry | suppressed by contrast | polyaxonal amacrine cell | vGluT3 amacrine cell | dual neurotransmission

In the vertebrate retina, different types of ganglion cells extract distinct features of the visual world and send different visual signals to various brain regions along parallel pathways (1–3). Complex receptive field properties of ganglion cells are shaped, to a large extent, by amacrine cells, which are an extremely diverse class of interneurons in the inner retina that regulate visual signal transmission from bipolar cells to ganglion cells. Signal processing by amacrine cells involves not only feed-forward interactions with ganglion cells and feedback interactions with bipolar cells but also mutual interactions among amacrine cells themselves (4–7). While amacrine–amacrine interactions have long been thought to provide a critical layer of network processing that enhances the computational capacity of the retina, the synaptic circuitry and functions of this layer of interactions are poorly understood in general.

Amacrine cells can be divided into three broad groups based on their arbor sizes in the inner plexiform layer (IPL) (4, 8). Small-field amacrines, many of which ramify diffusely in the IPL and release glycine, are believed to mediate mainly local and vertical (radial) interactions in the IPL. Wide-field amacrines, which tend to ramify narrowly and release GABA, are thought to mediate long-range, lateral interactions. Medium-field amacrines frequently ramify at multiple IPL depths and potentially mediate both lateral and vertical interactions. However, it is generally unclear how different groups of amacrine cells interact with each other in specific synaptic circuits. Moreover, it is unknown how such interactions influence the receptive fields and computational capabilities of amacrine cells and how these interactions provide an additional layer of network computation prior to signal integration by ganglion cells. To address these important questions, we investigated potential interactions between a small-field, diffusely stratified amacrine cell that expresses vGluT3 (vesicular glutamate transporter 3) (9–11) and a wide-field, polyaxonal amacrine cell (termed PAS4/5, see below) that ramifies narrowly at the border between sublaminae 4 (S4) and 5 (S5) of the IPL. The vGluT3 cell is a glutamatergic amacrine cell (GAC) that has been reported to release glutamate specifically onto ganglion cells specialized in detecting contrast, direction, and differential motion (12–14). GACs have also been shown to release glycine onto uniformity detectors (UD) (15, 16), a special class of ganglion cells that respond most vigorously to a uniform background, but are suppressed by local contrast signals—a trigger feature also known as suppressed-by-contrast (sbc) (15–26). We discovered a specific glycinergic synaptic pathway from GACs to PAS4/5 cells and showed that this pathway enables PAS4/5 cells to form an sbc receptive field. We further identified two subtypes of PAS4/5 cells based on their differences in synaptic connectivity and light response properties. Our results uncovered a synaptic circuit between a small-field and a wide-field amacrine cell. They revealed a role of the sbc

Significance

Interactions among amacrine cell types are critical for complex visual computation in the retina, but the underlying circuitry and functions are largely unknown. Here we report a specific pathway from small-field, dual-transmitter amacrine (vGluT3) to wide-field polyaxonal amacrine (PAS4/5) cells. This pathway mediates a characteristic form of glycinergic inhibition that is essential in shaping a suppressed-by-contrast (sbc) receptive field in PAS4/5 cells, thus representing one of the first few functionally identified interamacrine circuits. The existence of the sbc trigger feature upstream of ganglion cells suggests diverse functional roles of this fundamental form of circuit computation in multiple downstream circuits. The synaptic interactions between vGluT3 and PAS4/5 cells also illustrate a specific mechanism for feature-specific local control of global retina activity.

Author contributions: Y.J., S.L., Y.Z., and Z.J.Z. designed research; Y.J. performed research; Y.J., S.L., and Z.J.Z. analyzed data; and Z.J.Z. wrote the paper.

The authors declare no competing interest.

This article is a PNAS Direct Submission.

[1]To whom correspondence may be addressed. Email: jimmy.zhou@yale.edu or zhuoyh@mail.sysu.edu.cn.

This article contains supporting information online at https://www.pnas.org/lookup/suppl/doi:10.1073/pnas.1913417117/-/DCSupplemental.

First published April 9, 2020.

trigger feature in local control of global retinal activity. Preliminary results of this study have been reported in ref. 27.

Results

GACs Make Specific Glycinergic Synapses onto a Type of Polyaxonal Amacrine Cell. To understand interactions between GACs and wide-field amacrine cells, we searched for postsynaptic targets of GACs among displaced amacrine cells since most displaced amacrine cells are known to be wide-field GABAergic cells (28, 29). We used a whole-mount preparation of vGluT3-Cre-ChR2-EYFP mouse retina (12, 15), in which GACs are the only interneurons that selectively express channel rhodopsin 2 (ChR2). We optogenetically activated ChR2-expressing GACs with a flash of full-field blue light (referred to as blue light or optogenetic activation henceforth; *Materials and Methods*), while recording from small-soma (<12 μm in diameter) cells in the ganglion cell layer (GCL). We found that a population of polyaxonal amacrine cells responded to optogenetic activation of GACs with outward synaptic currents under voltage clamp at 0 mV (near cation reversal potential, E_{Cat}). These currents were activated within 4 to 8 ms ($n = 12$) of the onset of the blue light and persisted in the presence of a cocktail (20 μM L-2-amino-4-phosphonobutyric acid [L-AP4], 20 μM (*S*)-1-(2-Amino-2-carboxyethyl)-3-(2-carboxy-5-phenylthiophene-3-yl-methyl)-5-methylpyrimidine-2,4-dione [ACET], and 300 μM hexamethonium) that blocked light-evoked synaptic transmission from bipolar cells and cholinergic amacrine cells (12, 15) (Fig. 1*A*). They were resistant to ionotropic glutamate receptor antagonists 7-nitro-2,3-dioxo-1,2,3,4-tetrahydroquinoxaline-6-carbonitrile (CNQX) and 3-(2-Carboxypiperazin-4-yl)propyl-1-phosphonic acid (CPP) (20 and 40 μM, respectively, $n = 11$), the $GABA_A$ receptor antagonist SR95531 (SR, 50 μM, $n = 7$), and the gap junction blocker 18β-Glycyrrhetinic acid (18β-GA, 25 μM, $n = 5$, with 20-min perfusion), which were applied either individually or in combination (Fig. 1 *A* and *B*). However, these currents were completely blocked by strychnine (STR, 1 μM, $n = 5$; Fig. 1 *A* and *B*), indicating a direct glycinergic input from GACs. In the presence of the cocktail and 18β-GA (but without CNQX and CPP), the blue light-evoked postsynaptic currents had an I–V curve that reversed near −70 mV (near the Cl^- equilibrium potential, E_{Cl}; Fig. 1*C*), suggesting that this GAC input contained only a glycinergic component, even though GACs are known to release both glutamate and glycine. Notably, the amplitude of this postsynaptic glycinergic current varied from cell to cell, ranging from 20 to 200 pA at 0 mV ($n = 19$, see below).

The morphology of the above polyaxonal amacrine cells resembled that of WA4-1 (30), PA-S5 (28), and Rbp4 amacrine cells (RAC) (31) in mice, with dendrites and axons ramifying narrowly near the S4/S5 boarder in the IPL (Fig. 1 *D* and *E*). We term these cells PAS4/5. The dendrites of PAS4/5 were relatively thick and sparsely branched, forming a medium-size (~200 μm in radius) dendritic field. The axons of PAS4/5 were thin and varicose, extending up to ~1 mm in length. Some dendrites tapered down in caliber as they projected away from the soma and transformed into thin axons, but most axons either emanated from the soma or branched off abruptly from dendrites, often forming an obtuse angle with the dendrites (Fig. 1 *D* and *E*). PAS4/5 axons ramified only in the IPL and did not project to the GCL or the optic nerve head. The dendritic trees of PAS4/5 cells were decorated with numerous spines and intermittent appendages. Notably, some of these spines and appendages extended into the S4 layer and occasionally farther to the S3/S4 border, where they appeared to contact with GAC dendrites (*SI Appendix*, Fig. S1). Conversely, although GACs ramify predominantly between S2 and S3 layers, some of their distal dendritic tips protruded to S4 and even S4/S5 border of IPL and made contacts with the dendrites (especially dendritic spines) and, rarely, proximal axons of PAS4/5 cells (*SI Appendix*, Fig. S1). Thus, GACs and PAS4/5 seemed to specifically reach out to each other using the fine dendritic processes that extended out of their main arbors.

Receptive Field Properties of the Two PAS4/5 Cell Subtypes. To understand the receptive field properties of PAS4/5 cells, we first illuminated the retina with light spots of various sizes. We found two characteristically different types of light responses from PAS4/5 cells. Cells with type 1 light response characteristics (referred to as PAS4/5-1 henceforth) displayed maintained background spikes (under on-cell loose-patch recording) in the presence of a uniform, dark background. A center light spot of 100 μm radius (referred to as a small spot henceforth) evoked a transient suppression of the background spikes at the light onset (ON) and often a suppression of spikes at the light offset (OFF) as well (Fig. 2*A*). The transient ON spike suppression (recorded under on-cell loose patch clamp) corresponded to a transient membrane hyperpolarization (recorded under whole-cell current clamp; Fig. 2*A*) and a large transient ON inhibitory postsynaptic current (under whole-cell voltage clamp; Fig. 2*B*), suggesting that an ON center inhibitory input was responsible for the ON spike suppression. However, when the same PAS4/5-1 cell was stimulated by a 1,000-μm-radius light spot (referred to as a large spot henceforth), the transient ON spike suppression and the transient ON inhibitory input were greatly reduced, and the cell instead gave a robust ON response with a large increase in firing rate, suggesting that the inhibitory input to PAS4/5-1 cells was suppressed presynaptically by the large spot (Fig. 2 *A* and *B*). This spatial profile of the inhibitory input to PAS4/5-1 cells closely matched the GAC receptive field, which has a small excitatory center that is completely suppressible by a strong inhibitory surround of up to 1,000 μm in radius (12, 14, 15). The polarity of the inhibitory input to PAS4/5-1 cells (ON input only, no OFF; Fig. 2 *B* and *C*) also matched the local response polarity of GAC dendrites, which give ON responses in the ON sublamina and OFF responses in the OFF sublamina of the IPL (32, 33), consistent with a major contribution of GACs to the light-evoked inhibitory input to PAS4/5-1 cells. Notably, the above light response properties of PAS4/5-1 cells closely resemble the sbc receptive field properties of UDs (15–18, 20), which also receive a major glycinergic input from GACs (15, 16).

When a PAS4/5-1 cell was stimulated with a large spot, the spike suppression at light offset often remained. This OFF suppression was not associated with a postsynaptic inhibitory current input to PAS4/5-1 cells under either small- or large-spot stimulation (Fig. 2 *A* and *B*). Instead, it was often accompanied by a reduction in the excitatory input (seen as an outward shift in the baseline current at −70 mV and a reduction in baseline excitatory current noise; Fig. 2*B*), indicating a different underlying mechanism, most likely mediated by a presynaptic inhibition of bipolar cells as seen similarly with UDs (15).

The light-evoked excitatory synaptic input to PAS4/5-1 cells (under voltage clamp at −70 mV) was relatively small (Fig. 2*B*), similar in both size and kinetics to the light-evoked excitatory input to a UD (15). This excitatory input had an ON polarity presumably from ON bipolar cells terminating near S4/S5 layers since GACs did not make glutamatergic synapses onto PAS4/5-1 cells (Fig. 1 *A* and *C*). Unlike the light-evoked inhibitory input, which was greatly suppressed by a large spot, the ON excitatory input to a PAS4/5-1 was not suppressed by the large spot (Fig. 2*B*). Notably, although light spots evoked only a small excitatory input to PAS4/5-1 cells, the baseline holding current at −70 mV contained numerous small-amplitude background excitatory inputs, which likely contributed to the cells' spontaneous spiking and irradiance detection (see below).

The spatial profiles of light-driven excitatory and inhibitory inputs to PAS4/5-1 cells were further mapped with light annuli of various radii. Both the large inhibitory and small excitatory

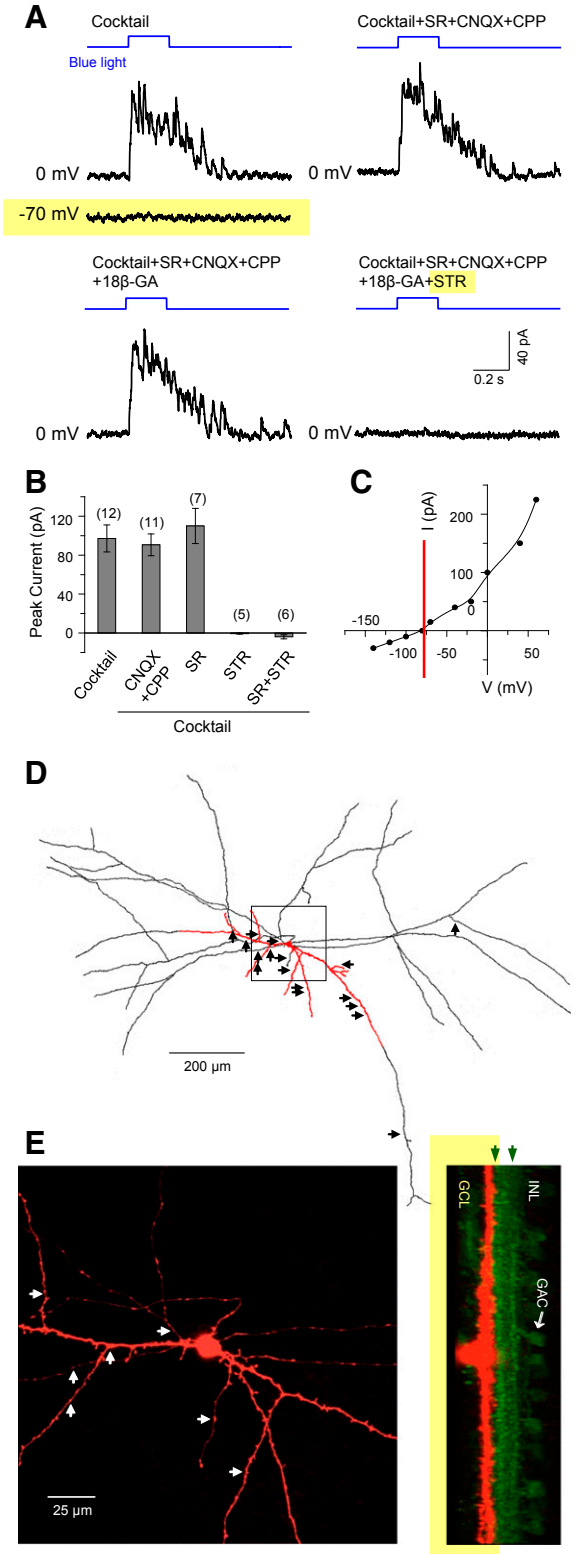

Fig. 1. Glycinergic synaptic input from GACs to PAS4/5 cells. (*A*) Responses of a voltage-clamped PAS4/5 cell to optogenetic (blue light) activation of GACs in physiological saline supplemented with a cocktail (20 μM L-AP4, 20 μM ACET, and 300 μM HEX), showing no response at −70 mV but outward currents at 0 mV (*Upper Left*) that were resistant to SR (50 μM), CNQX (40 μM), and CPP (20 μM) (*Upper Right*) and 18β-GA (25 μM with 20 min perfusion; *Lower Left*) but were completely blocked by STR (1 μM; *Lower Right*). (*B*) Summary of peak response amplitudes at 0 mV in various receptor blockers shown in *A*. Numbers in parentheses, cells tested. (*C*) I–V curve of optogenetically evoked currents in the presence of the cocktail and 18β-GA. (*D*) Tracing from a montage of two-photon image stacks taken from the PAS4/5 cell in *A*, showing putative dendrites (red) and axons (black). Arrow heads show putative contact points with GAC dendrites identified under two-photon imaging. (*E*) Expanded view of the demarcated area in *D*, showing tangential (*Left*) and cross-sectional (*Right*) views reconstructed from a two-photon image stack taken from the recorded PAS4/5 cell (red) in the vGluT3-Cre/ChR2-YFP retina (green). Green arrow heads in the cross-sectional view show locations corresponding to cholinergic bands.

inputs were confined within a center area of ∼200 μm in radius, matching the dendritic field size of PAS4/5 cells, with only a tiny inhibitory input at 0 mV and a transient suppression of the baseline excitatory input at −70 mV from areas outside the dendritic field (defined as the surround of a PAS4/5-1 cell) (Fig. 2*C*). Thus, unlike the center-excitatory, surround-inhibitory receptive field of most other retinal neurons, the receptive field of a PAS4/5-1 was dominated by a direct inhibitory input from the center, with no/little direct inhibition from its surround (Fig. 2*C*). Moreover, since the surround presynaptically suppressed the center inhibitory input to the PAS4/5-1 (Fig. 2*B*), the effective PAS4/5-1 receptive field could be characterized as being center-inhibitory, surround-disinhibitory/excitatory. This unusual receptive structure gave rise to the SBC trigger feature in PAS4/5-1s.

Cells with type 2 light response characteristics (referred to as PAS4/5-2 henceforth) also showed maintained spikes in a uniform dark background. However, in response to a small light spot, PAS4/5-2 rapidly generated robust ON spikes, without the initial transient suppression of spikes and the membrane hyperpolarization seen in PAS4/5-1 cells (Fig. 2*A*). A large spot evoked even more spikes in PAS4/5-2 cells, but the response profile remained similar to that elicited by a small spot (Fig. 2*A*). Thus, PAS4/5-2 cells lacked the sbc receptive field seen in PAS4/5-1 cells (Fig. 2 *A* and *D*). Voltage-clamp recording further showed that during a small-spot illumination, PAS4/5-2 cells received a much smaller inhibitory input than PAS4/5-1 cells did (Fig. 2*B*), resulting in an inhibitory charge transfer (at 0 mV) of 45 ± 9 pC ($n = 8$), compared to 141 ± 21 pC ($n = 8$, $P = 0.0010$) for PAS4/5-1 cells (Fig. 2*E*). The waveforms of light-evoked excitatory and inhibitory current inputs were also different between PAS4/5-1 and PAS4/5-2 (Fig. 2*B*), although the spatial extent of the inputs (center receptive field size) matched the dendritic field size in both subtypes (Fig. 2 *C* and *F*).

Notably, PAS4/5-2 cells received a much smaller direct glycinergic input from GACs than the PAS4/5-1 cells did. The peak postsynaptic response amplitudes to optogenetic activation of GACs were 124 ± 11 pA ($n = 10$) and 63 ± 12 pA ($n = 9$, $P = 0.0012$) in PAS4/5-1 and PAS4/5-2 cells, respectively (responses to optogenetic activation were measured after PAS4/5-1 and PAS4/5-2 cells had been identified based on their receptive field characteristics) (Fig. 2*G*). When data from both PAS4/5 subtypes were pooled together, we found a close correlation between the amplitude of optogenetically evoked GAC input and the amplitude of small-spot–evoked inhibitory input ($r^2 = 0.43$; Fig. 2*H*). Kernel density analysis showed that the pooled data fell into two separate clusters corresponding to the two subtypes of PAS4/5 cells (Fig. 2*I*). However, no consistent morphological difference was detected between PAS4/5-1 and PAS4/5-2 cells.

Contributions of GACs to the sbc Receptive Field Characteristics of PAS4/5-1s. Pharmacological experiments further showed that the majority of the small-spot–evoked inhibitory input to PAS4/5-1 cells was mediated by glycine receptors because STR (1 μM) blocked 83 ± 4% ($n = 4$) of the peak inhibitory input, whereas SR (50 μM) blocked only 15 ± 9.6% ($n = 4$) (Fig. 3 *A*, *B*, and *D*). In contrast, the light-evoked inhibitory input to a PAS4/5-2, which

NEUROSCIENCE

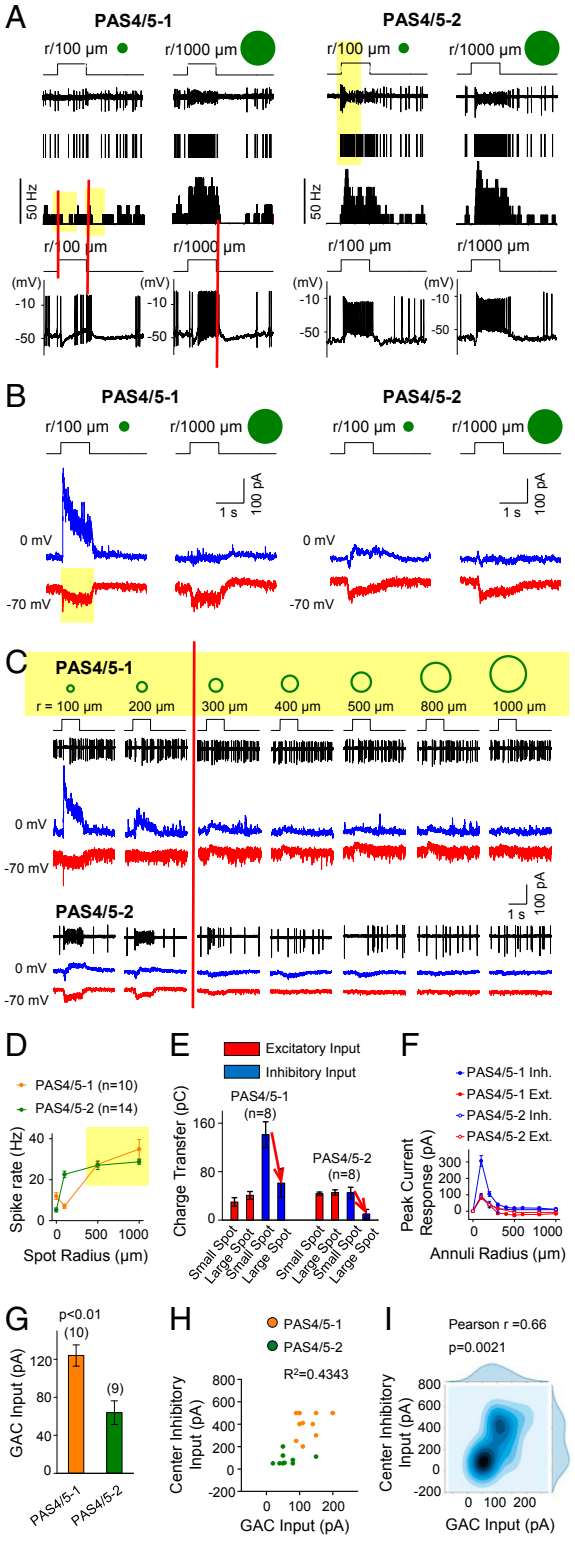

Fig. 2. Receptive field properties and synaptic connectivity of two subtypes of PAS4/5 cells. (*A*) (*Top*) Visual responses of a PAS4/5-1 and a PAS4/5-2 to small (100-µm radius) and large (1,000-µm radius) light spot illumination under on-cell loose-patch recording (first three rows show spike trains, raster plots, and spike rates, respectively) and whole-cell current-clamp recording (fourth row), showing transient sbc receptive field properties in the PAS4/5-1 but not the PAS4/5-2 cell. (*B*) Responses of a PAS4/5-1 and a PAS4/5-2 to small and large light spot illumination under whole-cell voltage clamp at 0 mV (blue) and −70 mV (red). (*C*) Responses of a PAS4/5-1 and a PAS4/5-2 to light annuli of various radii under on-cell loose-patch (*Top*) and whole-cell voltage-clamp recording (*Bottom*). Light annuli were 50 µm in thickness with outer radii denoted by r. (*D*) Mean spike rate (during the initial 0.5 s of the response to a light spot) as a function of spot radius, showing a spot size-dependent suppression of spikes in PAS4/5-1 but not PAS4/5-2 cells. (*E*) Charge transfer of excitatory and inhibitory current responses (integral of current responses at −70 and 0 mV, respectively) to small (100-µm radius) and large (1,000-µm radius) light spot stimulation. (*F*) Peak excitatory (at −70 mV) and inhibitory (at 0 mV) current responses of PAS4/5-1 (n = 6) and PAS4/5-2 cells (n = 6) in responses to light annuli of various radii. (*G*) Comparison of optogenetically evoked GAC input (peak current at 0 mV in the cocktail) between PAS4/5-1 (n = 10) and PAS4/5-2 (n = 9) cells. (*H*) Regression analysis of small-spot–evoked center inhibitory input and optogenetically evoked GAC input to PAS4/5-1 and PAS4/5-2 cells. R^2, coefficient of determination. (*I*) Kernel density analysis of same data shown in *H*.

was much smaller than that to a PAS4/5-1, was more sensitive to SR than to STR (Fig. 3 *A*, *B*, and *D*). STR also eliminated the transient ON spike suppression and the transient membrane hyperpolarization seen from PAS4/5-1 cells in response to a small-spot stimulation (Fig. 3*C*). In the presence of STR, the number of small-spot–evoked spikes in PAS4/5-1s increased dramatically, such that the response patterns to small- and large-spot illumination became similar (Fig. 3 *C* and *E*). On the other hand, PAS4/5-2 cells did not show a transient membrane hyperpolarization or spike suppression in response to the onset of a small light spot, and the specific effects of STR on the sbc response characteristics of PAS4/5-1 cells were not observed from PAS4/5-2 cells (Fig. 3 *C* and *E*). These results were consistent with a critical role of GACs in shaping the characteristic sbc receptive properties of PAS4/5-1 cells.

To illustrate the direct contribution of GACs to the characteristic sbc spike pattern of PAS4/5-1 cells, we investigated whether the glycinergic input from GACs alone was sufficient to produce the kind of spike suppression that mimics the characteristic sbc response of PAS4/5-1 cells under small-spot illumination. We first recorded PAS4/5-1 responses to a small light spot under current clamp in control (Fig. 3*F*, first trace). We then blocked all visually driven inputs to PAS4/5-1 cells with a cocktail (L-AP4, ACET, and HEX). To compensate for the significant reduction in PAS4/5-1 baseline spiking activity caused by the cocktail, we also injected a small step of depolarizing holding current (~50 pA) to PAS4/5-1 cells, so that they maintained a background spike rate similar to the spike rate in control (Fig. 3*F*, second trace). Under this condition, direct optogenetic activation of GACs alone (with a 1-s blue light flash) effectively induced in PAS4/5-1 cells a spike suppression and a membrane hyperpolarization (Fig. 3*F*, third trace) that mimicked the transient spike suppression and membrane hyperpolarization typically seen in the response to the onset of a small light spot in control (Fig. 3*F*, first trace). This direct suppressive effect of GACs on the PAS4/5-1 could be blocked by STR (Fig. 3*F*, fourth trace), confirming that the glycinergic input from GACs alone was sufficient to produce an ON spike suppression that mimicked the corresponding characteristic features of the sbc receptive field of PAS4/5-1 cells.

Kinetics of the GAC Input to PAS4/5-1 Cells. The light-evoked inhibitory input to a PAS4/5-1 was transient in kinetics (Fig. 4*A*, under voltage clamp). This transient inhibitory input produced only a transient suppression of the initial spike response to a prolonged (e.g., 20 s) stimulation by a small light spot, with little effect on the remaining sustained response (Fig. 4*B*, under current clamp). However, when the same light spot was flashed for the same prolonged period (20 s) at a higher temporal frequency (1 Hz), it evoked repetitive bursts of inhibitory current inputs (Fig. 4*C*, under voltage clamp), which were able to suppress the spike response throughout the prolonged stimulation duration (Fig. 4*D*, under current clamp). Increasing the light spot size (from 100 to 1,000 µm radius) reduced the spike suppression

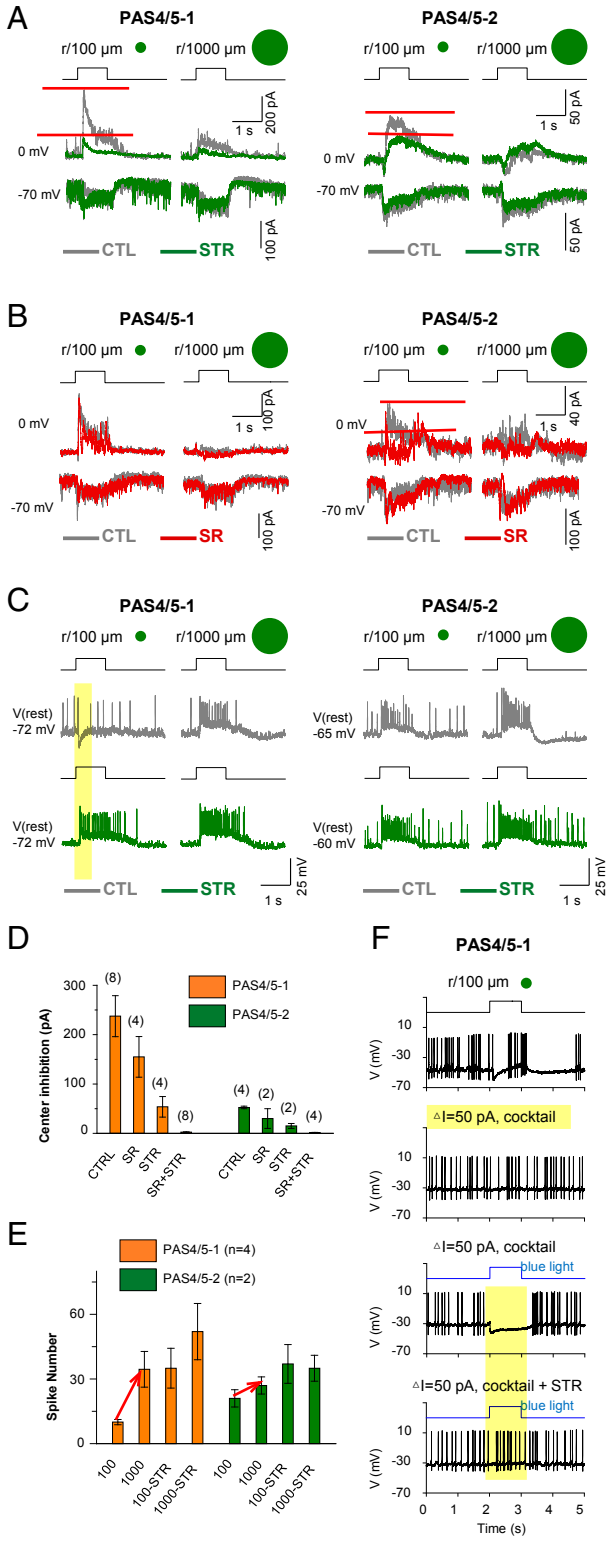

Fig. 3. Pharmacological properties of visually evoked and optogenetically evoked responses from PAS4/5-1 and PAS4/5-2 cells. (*A* and *B*) Effects of STR (1 µM; *A*) and SR (50 µM; *B*) on small (100-µm radius) and large (1,000-µm radius) spot-evoked synaptic inputs recorded under voltage clamp at 0 and −70 mV. Note the differences in scale bars between PAS4/5-1 and PAS4/5-2 cells. (*C*) Effects of STR on small and large-spot–evoked voltage responses of a PAS4/5-1 and a PAS4/5-2 under current clamp. (*D*) Summary of the effects of STR and SR on small-spot–evoked inhibitory currents in PAS4/5-1 and PAS4/5-2 cells. (*E*) Summary of STR effects on the number of spikes evoked by small and large spots during a 1-s illumination period. Number in parentheses in *D* and *E* indicate cells tested. (*F*) Comparison of visually evoked and optogenetically evoked spike suppression in a PAS4/5-1. The first trace shows voltage response to a 1-s visual (small spot) stimulation recorded under current clamp (at resting potential), showing a transient, light-evoked spike suppression associated with a membrane hyperpolarization. The second trace shows that in the presence of an antagonist cocktail (L-AP4, ACET, and HEX), the same cell was injected with a depolarizing current (50 pA) to evoke maintained spikes that resembled the spontaneous spikes shown in the first trace in control. The third trace shows optogenetic activation of GACs with a 1-s blue light flash (under the same condition as that of the second trace) evoked a spike suppression and a membrane hyperpolarization that mimicked the visually evoked sbc response seen in control (first trace). The fourth trace shows that STR completely blocked the optogenetically evoked spike suppression and membrane hyperpolarization.

during the prolonged, high-frequency light stimulation (Fig. 4 *E* and *F*), consistent with the GAC input being suppressed under the large-spot illumination (12, 14, 15). Similarly, STR also significantly reduced spike suppression during the prolonged, high-frequency stimulation by the small light spot (Fig. 4*E*), but it had a much less effect on the spike responses to high-frequency stimulation by a large spot (Fig. 4*F*), presumably because the glycinergic input from GACs was already suppressed by the large light spot. Together, the above results suggested that the inhibition from GACs to PAS4/5-1s was tuned to spatially contrasting and temporally varying stimuli.

Irradiance-Encoding Responses of PAS4/5 Cells. We also examined the responses of PAS4/5 cells to full-field, uniform light of various intensities, an illumination condition where the GAC input was expected to be largely suppressed. Both PAS4/5-1 and PAS4/5-2 cells displayed sustained spikes in response to uniform light illumination, with spike rates that were proportional to the light intensity (Fig. 5 *A* and *B*), thus demonstrating an irradiance-encoding ability similar to that recently reported for RAC cells in Rbp4-Cre mice (31). However, the two PAS4/5 subtypes had different irradiance-encoding characteristics. Compared to PAS4/5-2s, PAS4/5-1s displayed a higher steady-state firing rate at all irradiance levels tested (Fig. 5 *A* and *B*). The steady-state irradiance response curve of PAS4/5-1s had a steeper dependence on irradiance and did not reach a saturation plateau even at the highest irradiance level tested ($10^{16.5}$ photons cm^{-2} s^{-1}), whereas that of PAS4/5-2s had a much shallower irradiance dependence and reached a response plateau at $10^{15.5}$ photons cm^{-2} s^{-1} (Fig. 5*B*). The irradiance response kinetics was also different between the two PAS4/5 subtypes. In response to a step increment in uniform irradiance, PAS4/5-1s immediately increased their firing rates to a relatively stable, irradiance-dependent level, whereas PAS4/5-2 cells increased their firing rates to an initial peak level, followed by a gradual decline in firing rate to a lower, irradiance-dependent, steady-state level within 5 to 10 s (Fig. 5*C*). A comparison with the reported irradiance-encoding properties of RACs (31) suggested that the PAS4/5-2 had a closer resemblance to RACs than PAS4/5-1s did.

Discussion

This study revealed a new synaptic pathway from GACs to PAS4/5-1, thus providing one of the few examples of functionally identified interamacrine microcircuits (5, 34). The presence of this pathway was rather unexpected because GACs and PAS4/5s ramified mainly at different IPL depths. Our results suggested that the contacts between the distal dendritic tips of GACs and the fine dendritic structures (spines and appendages) of PAS4/5-1s, although infrequent, were specific and played a functional role. The synapses from GACs to PAS4/5-1s were solely glycinergic even though GACs are known to release both glutamate and glycine, suggesting that GACs make segregated glycinergic

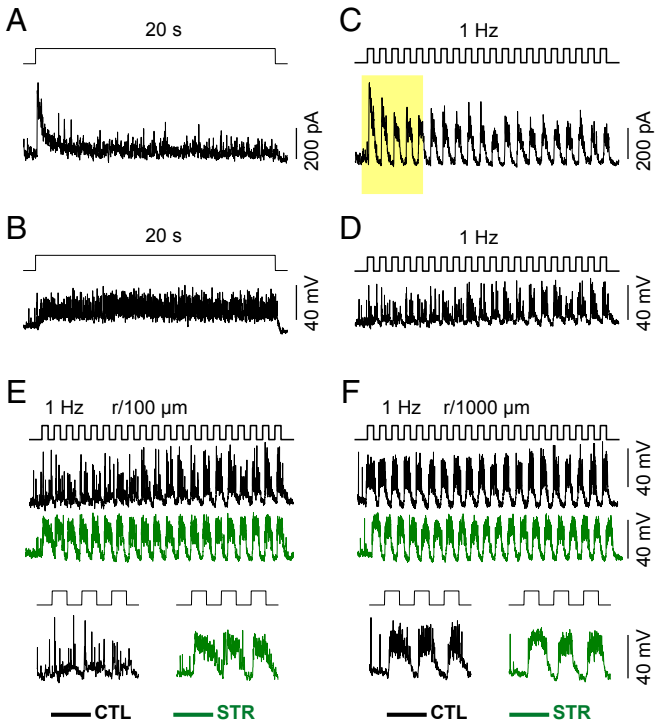

Fig. 4. Temporal dynamics of the glycinergic input to PAS4/5-1 cells. (*A* and *B*) Inhibitory current and voltage responses of a PAS4/5-1 to a prolonged (20-s) stimulation of a small (100-μm radius) center light spot, showing a transient inhibitory current input (*A*; voltage-clamped at 0 mV) and a transient suppression of spikes (*B*; current-clamped at the resting potential −74 mV) at the onset of the stimulation. (*C* and *D*) Responses to same duration of stimulation as in *A* and *B* but at a higher temporal frequency (1 Hz), showing repetitive bursts of inhibitory current inputs that persisted the entire stimulation duration (*C*) and repetitive bursts of spike responses that were suppressed at the onset of each burst (*D*). (*E*) The spike responses to the flickering small-spot stimulation in *D* (black trace) were greatly enhanced by STR (1 μM; green trace), as shown more clearly in the expanded panels at the bottom, suggesting a significant suppression of spikes by a glycinergic drive in the control solution. (*F*) Responses to 1-Hz flickering of a large (1,000-μm radius) light spot, showing an increased spike rate in the control solution (black trace) compared to the response to the small flickering spot (*D*) and a lack of significant effect of STR on the spike rate (green trace), as seen more clearly in the expanded panels at the bottom.

and glutamatergic outputs to separate postsynaptic circuits, as with all of the ganglion cells so far identified as postsynaptic targets of GACs (15, 16). However, it remains to be determined whether there are other amacrine cell types, which receive both glutamatergic and glycinergic inputs from GACs. In the brain, neurons expressing vGluT3 often corelease glutamate and a different classic transmitter (35), such as acetylcholine, GABA, and serotonin (36–38). While glutamate-GABA cotransmission has been reported at vGluT2-expressing synapses from entopeduncular nucleus to lateral habenula, functional evidence for cotransmission at single vGluT3-expressing synapses is still lacking (37).

Because GACs have a small-center, strong-surround antagonistic receptive field structure and are sensitive to relative motion (12, 14), their glutamatergic output is expected to enhance the contrast and motion sensitivity of their postsynaptic target cells. On the other hand, the glycinergic output from GACs does the opposite: it shapes a center-inhibitory, surround-disinhibitory receptive field, which plays a crucial role in generating the sbc trigger feature in PAS4/5-1 cells. A similar role of the glycinergic input from GACs has been reported for UDs (15, 16). We also identified a subpopulation of PAS4/5 cells that received only a weak input from GACs. That the PAS4/5-2 subpopulation lacked an obvious sbc receptive field structure, in turn, further supports a critical role of GACs in shaping the sbc receptive field of PAS4/5-1s. On the other hand, because the visually (small spot) evoked inhibitory input to a PAS4/5-1 was often considerably larger in amplitude than the total optogenetically evoked glycinergic input from GACs (Figs. 2 and 3), it is likely that other amacrine cells, especially other small-field amacrine cells, also contributed to the center inhibitory input to and the sbc receptive field of PAS4/5-1s.

Our results demonstrated that the sbc trigger feature can be generated in a retinal circuit presynaptic to ganglion cells, suggesting that this form of visual processing occurs more widely in the retina than previously thought. Suppression of background firing by the onset and offset of a contrast change in the receptive center (sbc) is considered one of the four

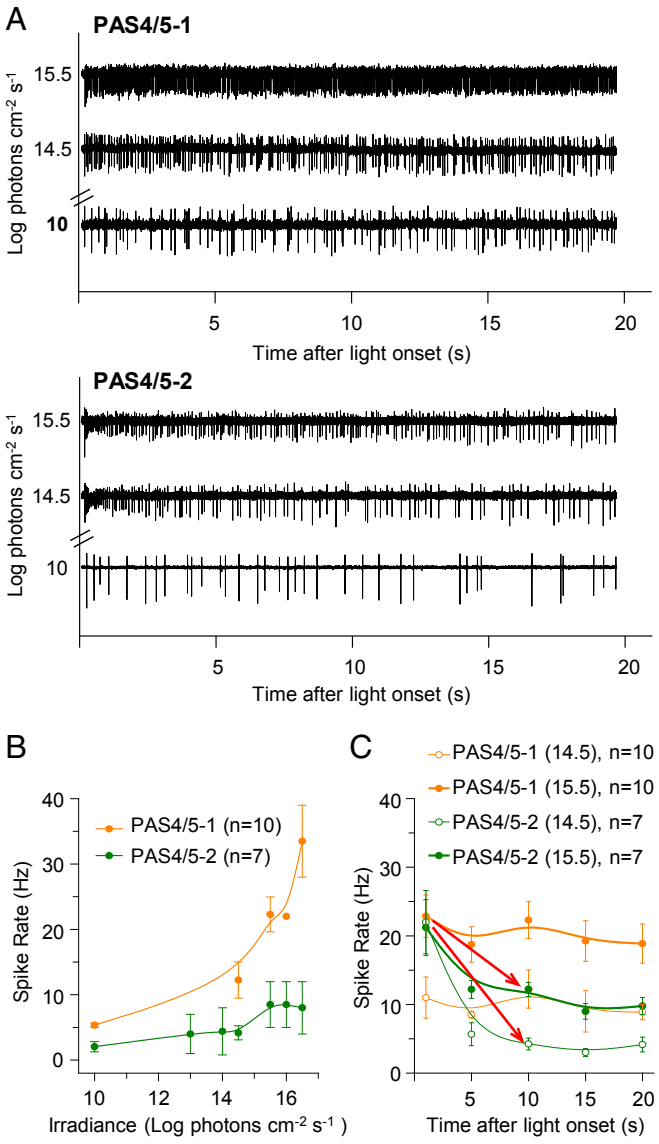

Fig. 5. Irradiance-encoding properties of PAS4/5-1 and PAS4/5-2 cells. (*A*) On-cell loose-patch recording of a PAS4/5-1(*Upper*) and a PAS4/5-2(*Lower*) in response to a series of whole-field light steps of various irradiances. (*B*) Irradiance response curves of steady-state responses (spike rates measured at 10 s after light onset) of PAS4/5-1 and PAS4/5-2 cells. (*C*) Comparison of temporal properties of irradiance responses (spike rates) of PAS4/5-1 and PAS4/5-2 cells following step increments of uniform irradiance to $10^{14.5}$ and $10^{15.5}$ photons cm^{-2} s^{-1}.

fundamental trigger features regarding light response polarity (20). It is distinct from the other three fundamental trigger features (activation of firing by the onset, offset, and on-offset of a contrast change, respectively). Similar sbc receptive field properties have also been reported in dorsal lateral geniculate nucleus (39) and visual cortex (40), suggesting a basic trigger feature in the central visual system. By building an sbc receptive structure in an amacrine cell circuit upstream to retinal output neurons, PAS4/5-1 cells may use this fundamental trigger feature to shape the receptive fields of multiple downstream circuits, thereby achieving more computational capabilities. For example, in cells that receive a GABAergic input from PAS4/5-1s, an sbc response of PAS4/5-1 cells may cause a transient suppression of GABAergic inhibition (i.e., a disinhibition), resulting in a transient excitatory response to local contrast and/or relative object motion. Amacrine cells with PAS4/5-like morphology have been shown to be electrically coupled to other cells (41), including ipRGCs (31, 42, 43). In those gap junction-coupled cells, an sbc response of PAS4/5-1s may lead to a transient suppression of cell excitability. We also found that PAS4/5-1s and PAS4/5-2s are irradiance detectors, with different irradiance response properties. That GACs selectively inhibit cells involved in encoding uniformity and luminosity is intriguing and requires further investigation.

Finally, this study illustrates how crosstalk between different amacrine cell classes enhances visual processing in the inner retina. It is generally believed that narrow-field, diffusely stratified amacrine cells mediate local interactions across different IPL sublayers, whereas wide-field amacrine cells mediate global lateral interactions. Our results now demonstrate that the long-range output of PAS4/5-1 cells, which is tuned to spatially uniform and temporally sustained illumination, can be effectively suppressed by the narrow-field inhibition from GACs, which is tuned to local contrast changes and relative motion. This finding revealed a specific circuit mechanism, through which a narrow-field amacrine cell regulates global retinal activity as far as a millimeter away.

Materials and Methods

All animal procedures were performed in accordance with National Institutes of Health guidelines. vGluT3-Cre/ChR2-YFP mice were generated by cross-breeding vGluT3 Cre mice (strain: Tg(Slc17a8-icre)1Edw, JAX: 018147, Jackson Laboratory; RRID: IMSR_JAX:018147) (9, 12) with ChR2-YFP mice (strain B6;129S-*Gt(ROSA)26Sor*$^{tm32(CAG-COP4*H134R/EYFP)Hze}$/J, Jackson Laboratory; RRID: IMSR_JAX: 012569). A flat-mount retinal preparation was prepared under dim red light illumination and studied with optogenetic activation, patch clamp recording, and two-photon imaging as previously described (12, 15, 32). Detailed materials and methods are described in *SI Appendix*.

Data Availability Statement. All relevant data are included in the manuscript and *SI Appendix*.

ACKNOWLEDGMENTS. We thank Minggang Chen for help with data analysis. This work was supported in part by NIH grants R01EY026065 (Z.J.Z.) and P30EY026878 (to Yale Vision Core); Research to Prevent Blindness, Inc. unrestricted grant to Yale Eye Center; Marvin L. Sears Endowed Professorship (Z.J.Z.); and a training scholarship from International Program for Ph.D. Candidates, Sun Yat-Sen University (Y.J.).

1. T. Baden *et al*., The functional diversity of retinal ganglion cells in the mouse. *Nature* **529**, 345–350 (2016).
2. J. R. Sanes, R. H. Masland, The types of retinal ganglion cells: Current status and implications for neuronal classification. *Annu. Rev. Neurosci.* **38**, 221–246 (2015).
3. A. D. Huberman, C. M. Niell, What can mice tell us about how vision works? *Trends Neurosci.* **34**, 464–473 (2011).
4. J. S. Diamond, Inhibitory interneurons in the retina: Types, circuitry, and function. *Annu. Rev. Vis. Sci.* **3**, 1–24 (2017).
5. S. Lee, Z. J. Zhou, The synaptic mechanism of direction selectivity in distal processes of starburst amacrine cells. *Neuron* **51**, 787–799 (2006).
6. M. Helmstaedter *et al*., Connectomic reconstruction of the inner plexiform layer in the mouse retina. *Nature* **500**, 168–174 (2013).
7. K. Franke, T. Baden, General features of inhibition in the inner retina. *J. Physiol.* **595**, 5507–5515 (2017).
8. R. H. Masland, The tasks of amacrine cells. *Vis. Neurosci.* **29**, 3–9 (2012).
9. W. N. Grimes, R. P. Seal, N. Oesch, R. H. Edwards, J. S. Diamond, Genetic targeting and physiological features of VGLUT3+ amacrine cells. *Vis. Neurosci.* **28**, 381–392 (2011).
10. J. Johnson *et al*., Vesicular glutamate transporter 3 expression identifies glutamatergic amacrine cells in the rodent retina. *J. Comp. Neurol.* **477**, 386–398 (2004).
11. S. Haverkamp, H. Wässle, Characterization of an amacrine cell type of the mammalian retina immunoreactive for vesicular glutamate transporter 3. *J. Comp. Neurol.* **468**, 251–263 (2004).
12. S. Lee *et al*., An unconventional glutamatergic circuit in the retina formed by vGluT3 amacrine cells. *Neuron* **84**, 708–715 (2014).
13. A. Krishnaswamy, M. Yamagata, X. Duan, Y. K. Hong, J. R. Sanes, Sidekick 2 directs formation of a retinal circuit that detects differential motion. *Nature* **524**, 466–470 (2015).
14. T. Kim, F. Soto, D. Kerschensteiner, An excitatory amacrine cell detects object motion and provides feature-selective input to ganglion cells in the mouse retina. *eLife* **4**, 1–15 (2015).
15. S. Lee, Y. Zhang, M. Chen, Z. J. Zhou, Segregated glycine-glutamate co-transmission from vGluT3 amacrine cells to contrast-suppressed and contrast-enhanced retinal circuits. *Neuron* **90**, 27–34 (2016).
16. N. W. Tien, T. Kim, D. Kerschensteiner, Target-specific glycinergic transmission from VGluT3-expressing amacrine cells shapes suppressive contrast responses in the retina. *Cell Rep.* **15**, 1369–1375 (2016).
17. W. R. Levick, Receptive fields and trigger features of ganglion cells in the visual streak of the rabbits retina. *J. Physiol.* **188**, 285–307 (1967).
18. B. Sivyer, W. R. Taylor, D. I. Vaney, Uniformity detector retinal ganglion cells fire complex spikes and receive only light-evoked inhibition. *Proc. Natl. Acad. Sci. U.S.A.* **107**, 5628–5633 (2010).
19. R. W. Rodieck, Receptive fields in the cat retina: A new type. *Science* **157**, 90–92 (1967).
20. J. Jacoby, G. W. Schwartz, Typology and circuitry of suppressed-by-contrast retinal ganglion cells. *Front. Cell. Neurosci.* **12**, 269 (2018).
21. D. N. Mastronarde, Two types of cat retinal ganglion cells that are suppressed by contrast. *Vision Res.* **25**, 1195–1196 (1985).
22. F. M. de Monasterio, Properties of ganglion cells with atypical receptive-field organization in retina of macaques. *J. Neurophysiol.* **41**, 1435–1449 (1978).
23. J. B. Troy, G. Einstein, R. P. Schuurmans, J. G. Robson, C. Enroth-Cugell, Responses to sinusoidal gratings of two types of very nonlinear retinal ganglion cells of cat. *Vis. Neurosci.* **3**, 213–223 (1989).
24. B. Sivyer, D. I. Vaney, Dendritic morphology and tracer-coupling pattern of physiologically identified transient uniformity detector ganglion cells in rabbit retina. *Vis. Neurosci.* **27**, 159–170 (2010).
25. N. W. Tien, J. T. Pearson, C. R. Heller, J. Demas, D. Kerschensteiner, Genetically identified suppressed-by-contrast retinal ganglion cells reliably signal self-generated visual stimuli. *J. Neurosci.* **35**, 10815–10820 (2015).
26. J. Jacoby, Y. Zhu, S. H. DeVries, G. W. Schwartz, An amacrine cell circuit for signaling steady illumination in the retina. *Cell Rep.* **13**, 2663–2670 (2015).
27. Y. Jia, S. Lee, Y. Zhuo, Z. J. Zhou, A retinal circuit for local suppression of wide-field inhibition. *Invest. Ophthalmol. Vis. Sci.* **59**, 1 (2018).
28. L. Pérez De Sevilla Müller, J. Shelley, R. Weiler, Displaced amacrine cells of the mouse retina. *J. Comp. Neurol.* **505**, 177–189 (2007).
29. S. Majumdar, J. Weiss, H. Wässle, Glycinergic input of widefield, displaced amacrine cells of the mouse retina. *J. Physiol.* **587**, 3831–3849 (2009).
30. B. Lin, R. H. Masland, Populations of wide-field amacrine cells in the mouse retina. *J. Comp. Neurol.* **499**, 797–809 (2006).
31. S. Sabbah, D. Berg, C. Papendorp, K. L. Briggman, D. M. Berson, A Cre mouse line for probing irradiance- and direction-encoding retinal networks. *eNeuro* **4**, ENEURO.0065–17.2017 (2017).
32. M. Chen, S. Lee, Z. J. Zhou, Local synaptic integration enables ON-OFF asymmetric and layer-specific visual information processing in vGluT3 amacrine cell dendrites. *Proc. Natl. Acad. Sci. U.S.A.* **114**, 11518–11523 (2017).
33. J. C. Hsiang, K. P. Johnson, L. Madisen, H. Zeng, D. Kerschensteiner, Local processing in neurites of VGluT3-expressing amacrine cells differentially organizes visual information. *eLife* **6**, e31307 (2017).
34. X. Huang, M. Rangel, K. L. Briggman, W. Wei, Neural mechanisms of contextual modulation in the retinal direction selective circuit. *Nat. Commun.* **10**, 2431 (2019).
35. S. El Mestikawy, A. Wallén-Mackenzie, G. M. Fortin, L. Descarries, L. E. Trudeau, From glutamate co-release to vesicular synergy: Vesicular glutamate transporters. *Nat. Rev. Neurosci.* **12**, 204–216 (2011).
36. C. Gras *et al*., The vesicular glutamate transporter VGLUT3 synergizes striatal acetylcholine tone. *Nat. Neurosci.* **11**, 292–300 (2008).
37. J. Noh, R. P. Seal, J. A. Garver, R. H. Edwards, K. Kandler, Glutamate co-release at GABA/glycinergic synapses is crucial for the refinement of an inhibitory map. *Nat. Neurosci.* **13**, 232–238 (2010).
38. A. Belmer *et al*., Axonal non-segregation of the vesicular glutamate transporter VGLUT3 within serotonergic projections in the mouse forebrain. *Front. Cell. Neurosci.* **13**, 193 (2019).
39. D. M. Piscopo, R. N. El-Danaf, A. D. Huberman, C. M. Niell, Diverse visual features encoded in mouse lateral geniculate nucleus. *J. Neurosci.* **33**, 4642–4656 (2013).
40. C. M. Niell, M. P. Stryker, Highly selective receptive fields in mouse visual cortex. *J. Neurosci.* **28**, 7520–7536 (2008).
41. B. Völgyi, S. Chheda, S. A. Bloomfield, Tracer coupling patterns of the ganglion cell subtypes in the mouse retina. *J. Comp. Neurol.* **512**, 664–687 (2009).
42. L. P. Müller, M. T. Do, K. W. Yau, S. He, W. H. Baldridge, Tracer coupling of intrinsically photosensitive retinal ganglion cells to amacrine cells in the mouse retina. *J. Comp. Neurol.* **518**, 4813–4824 (2010).
43. A. N. Reifler *et al*., All spiking, sustained ON displaced amacrine cells receive gap-junction input from melanopsin ganglion cells. *Curr. Biol.* **25**, 2763–2773 (2015).